Purdue University
Purdue e-Pubs

Purdue Energetics Research Center Articles | Purdue Energetics Research Center

5-2012

Feasibility Study and Demonstration of an Aluminum and Ice Solid Propellant

Timothee L. Pourpoint
Purdue University, timothee@purdue.edu

Tyler D. Wood
Purdue University

Mark A. Pfeil
Purdue University

John Tsohas
Purdue University

Steven F. Son
Purdue University

Follow this and additional works at: https://docs.lib.purdue.edu/perc_articles

Recommended Citation
Timothee L. Pourpoint, Tyler D. Wood, Mark A. Pfeil, John Tsohas, and Steven F. Son, "Feasibility Study and Demonstration of an Aluminum and Ice Solid Propellant," International Journal of Aerospace Engineering, vol. 2012, Article ID 874076, 11 pages, 2012. doi:10.1155/2012/874076

This document has been made available through Purdue e-Pubs, a service of the Purdue University Libraries. Please contact epubs@purdue.edu for additional information.

Hindawi Publishing Corporation
International Journal of Aerospace Engineering
Volume 2012, Article ID 874076, 11 pages
doi:10.1155/2012/874076

Research Article

Feasibility Study and Demonstration of an Aluminum and Ice Solid Propellant

Timothee L. Pourpoint, Tyler D. Wood, Mark A. Pfeil, John Tsohas, and Steven F. Son

School of Aeronautics and Astronautics, Purdue University, 500 Allison Road, West Lafayette, IN 47907, USA

Correspondence should be addressed to Timothee L. Pourpoint, timothee@purdue.edu

Received 11 March 2012; Accepted 25 May 2012

Academic Editor: Valsalayam Sanal Kumar

Copyright © 2012 Timothee L. Pourpoint et al. This is an open access article distributed under the Creative Commons Attribution License, which permits unrestricted use, distribution, and reproduction in any medium, provided the original work is properly cited.

Aluminum-water reactions have been proposed and studied for several decades for underwater propulsion systems and applications requiring hydrogen generation. Aluminum and water have also been proposed as a frozen propellant, and there have been proposals for other refrigerated propellants that could be mixed, frozen in situ, and used as solid propellants. However, little work has been done to determine the feasibility of these concepts. With the recent availability of nanoscale aluminum, a simple binary formulation with water is now feasible. Nanosized aluminum has a lower ignition temperature than micron-sized aluminum particles, partly due to its high surface area, and burning times are much faster than micron aluminum. Frozen nanoscale aluminum and water mixtures are stable, as well as insensitive to electrostatic discharge, impact, and shock. Here we report a study of the feasibility of an nAl-ice propellant in small-scale rocket experiments. The focus here is not to develop an optimized propellant; however improved formulations are possible. Several static motor experiments have been conducted, including using a flight-weight casing. The flight weight casing was used in the first sounding rocket test of an aluminum-ice propellant, establishing a proof of concept for simple propellant mixtures making use of nanoscale particles.

1. Introduction

Aluminum powder is a common ingredient in conventional solid rocket propellants. It is used to increase specific impulse, I_{sp}, as well as stability. The properties and recent availability of nanoscale aluminum (nAl) have motivated recent efforts in new solid propellant formulations. For example, Kuo et al. [1] discussed the potential use of nanosized powders for rocket propulsion in a recent paper. Many of the potential advantages listed for these particles are short ignition delay, fast burning times, and the possibility to act as an energetic gelling agent. Using nAl has been shown to produce a significant increase in performance with conventional solid propellants [2, 3]. Researchers showed that replacing 50 μm particles with the same amount of nominally 100 nm particles in AP-based propellants could result in a burning rate increase of up to 100% [4]. Most of these characteristics can be attributed to the high-specific surface area of the nanoscale particles [1, 5]. The possible drawbacks of nAl are the reduction in active aluminum content, electrostatic discharge (ESD) sensitivity when dry, and poor rheological properties. Other research has been conducted pairing this increased reactivity of nAl with less reactive oxidizers such as water in addition to conventional oxidizers [6, 7]. Aluminum and water propellants may prove to be suited for deep space exploration in that propellants could be made in situ from available water and aluminum. Also, the products of this propellant, mainly H_2 and Al_2O_3, are relatively nontoxic, making it a "greener" propellant [8, 9].

The objectives of this paper are to present results of nAl/ice (ALICE) small-scale static experiments, along with the launch of a sounding rocket powered by ALICE. Another objective was to develop larger scale (kilogram scale) mixing procedures that produce a consistent material. A classical mixer and a newly available Resodyn mixer were considered. The burning rate was characterized for these propellants in

a strand burner. Results of the static test firings are also compared against internal ballistic predictions.

2. Background

While bulk commercial nAl has only recently been developed, the water-aluminum reaction received attention as early as the 1940s. In 1942, Rasor and Portland [10] filed a patent, which proposed to use seawater and aluminum to propel a submarine. While thermodynamically this reaction would be viable, the kinetics of the available aluminum would not yield complete reaction. This was evident by work done by Elgert and Brown [11] who used U235 to melt the aluminum but could only react 0.2% of the aluminum, even though temperatures reached ~1200°C. Even work done by Leibowitz and Mishler [12], who tried igniting aluminum with a laser, found that if the melting temperature of the aluminum oxide was not reached, ignition would not occur.

Several studies investigated the use of micron-sized Al powders with water for underwater propulsion [13, 14]. In 2004, Ingenito and Bruno [8] also published a paper discussing the potential uses for an aluminum-water mixture for space propulsion. Using the NASA CEA equilibrium code, they calculated the theoretical specific impulse values of mixtures over a range of oxidizer-to-fuel (O/F) ratios. Assuming an expansion ratio of 100, the calculated vacuum I_{sp} at an O/F of ~1.2 is greater than 300 s and higher than that of most solid propellants [15]. Ingenito and Bruno also proposed the idea of adding hydrogen peroxide (H_2O_2) to increase performance. Indeed, many other propellant formulations are possible [8].

Nanoscale aluminum can dramatically increase the reaction rates of aluminum and water. Ivanov et al. [16] reported the earliest combustion work with stoichiometric mixtures of nAl and water. They reported needing 3% polyacrylamide to thicken (or gel) the water and enable the nAl-water reaction. In 2006, Risha et al. [17] reported, for the first time, the combustion of nAl and water without the use of a gelling agent. Risha's successful results were likely attributable to a higher surface area nAl than previously used. Risha et al. found that stoichiometric mixtures of nAl-water propellant have a pressure dependence of around 0.47 and have densities of around 1.5 g/cm^3. While the burning rate for a fuel-lean mixture was lower than a stoichiometric mixture, the pressure exponents were similar. This suggests that the propellant has the same pressure dependence, regardless of the amount of excess water.

Upon production by manufacturers, such as Novacentrix Inc. and Argonide Corp, aluminum powders form a passivation layer of alumina. Even with this passivation layer, nAl-water can have a short shelf life, on the order of weeks, when exposed to moist air due to the high affinity of nAl for oxygen [18]. The inert alumina shell adversely affects the performance of the mixture [5, 17]. Due to the smaller size of the aluminum particles (from micron to nano), the alumina layer accounts for more of the mass in nAl particles. Dokhan et al. [19] estimate that active aluminum content of micron aluminum is 99.5% or better, while the active aluminum content of passivated nAl typically ranges from 50% to 95% [18, 20, 21].

Franson et al. [22] performed perhaps the first work on the implementation of ALICE in a rocket motor configuration. The outer diameter of the grain was 86 mm, with an inner perforation diameter of 60 mm and a length of 157 mm. The total mass of the grain using a combination of micron and nanoscale aluminum was 550 g. Postinspection of the motor revealed large amounts of alumina residues in the chambers. Analysis of the slag showed that ~17% of the initial aluminum did not participate in the reaction. This helped explain the observed maximum pressure of 1.6 MPa compared to the 3 MPa expected value.

In previous work by our group, we examined the aging characteristics of aluminum and water mixtures. One method to increase shelf life is to freeze the aluminum water mixture to form ALICE. Sippel et al. [18] showed that nAl and water stored at −25°C retained its original active aluminum content after 40 days, following a procedure by Cliff et al. [21]. This was a significant increase from the previous findings that had a value less then 10% after the same time period in liquid water. In addition, Sippel et al. found that over the course of six months, the active aluminum content was unchanged within the uncertainty of the measurement [18].

Safety testing was also performed on the experimental propellant. Impact sensitivity testing showed that a mixture of frozen nAl using nominally 80 nm powder and water (ALICE) has a drop height greater than the capacity of the experiment apparatus (>2.2 meters), while dry 200 μm AP has a drop height of 38.5 cm. ESD testing showed that stoichiometric ALICE mixtures have an energy threshold greater than 1.5 J, over one thousand times the amount of energy typically released in a human ESD event. Shock sensitivity was performed to determine whether the propellant would propagate a detonation wave. The results displayed the stability of the frozen propellant using 80 nm nAl, with no indication of damage to a witness plate [18].

3. Mixing Techniques

Early mixtures in this work were mixed by hand or using a Ross DPM-1Q dual planetary mixer (Charles Ross & Son Company, Hauppauge, New York). However, inconstancies in mixing and packing densities motivated other approaches. A Resodyn LabRAM resonating mixer (Resodyn Acoustic Mixer Inc., Butte, Montana) was ultimately selected to mix the ALICE propellant. The LabRAM mixer is designed to operate at the resonant frequency of the system being mixed, using the user-specified intensity (ranging from 0 to 100) [23]. The density and viscosity of the system will change as it mixes causing the resonant frequency of the system and the energy put into the mixture (measured by the acceleration level) to change with time.

The changes in acceleration and frequency provide important information related to the completeness of the mixing process. In a typical mix, the frequency of the mixer increases initially and then drops, while the acceleration

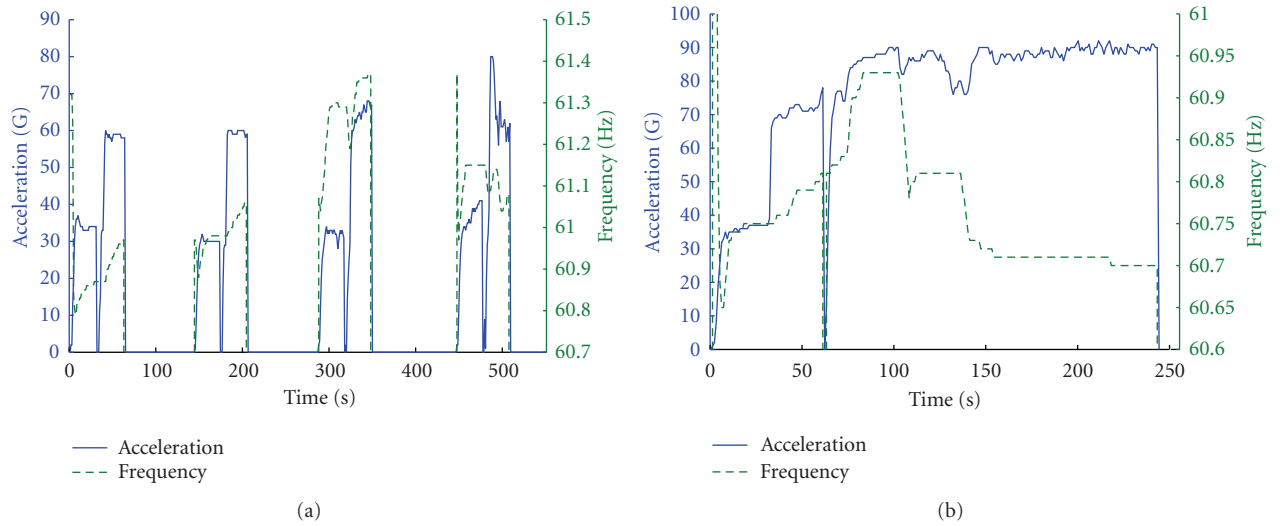

Figure 1: Traces from the Resodyn mixer: (a) acceleration and frequency of consecutive multiple mixing cycles; (b) acceleration and frequency of single mixing cycle of near constant intensity.

Figure 2: Images of various stages of mixing in 7.6 cm (3″) diameter jar: (a) mixing consistency after first cycle; (b) mixing consistency after second cycle; (c) mixing consistency after final cycle.

exhibits a general continual increase. These fluctuations occur due to the changing mixture properties throughout mixing (Figure 1).

As shown in Figure 2(a), ALICE starts out as a mixture of deionized water and 80 nm aluminum powder from Novacentrix Inc. (Product no.: M2666, properties listed in Table 1). Upon mixing, the mixture begins to form clumps until it becomes a uniform paste-like substance (Figure 2(b)). The properties of the propellant then reach a uniform state; in other words the propellant is fully mixed, when the acceleration and the frequency level off for a period of time (Figure 2(c)).

4. Burning Rate Measurements Technique and Results

In previous work with the Ross dual planetary mixer, stoichiometric mixtures proved to be too viscous for the size of nAl used. The propellant became too thick to mix effectively with the Ross mixer. This viscous behavior prompted the final ALICE mixtures to be fuel-lean with a target equivalence ratio, ϕ, of 0.75. Fuel-lean mixtures had an overall decrease in burning rate when compared to stoichiometric mixtures, but Risha et al. show similar pressure exponents for both the fuel-lean and stoichiometric mixtures [17].

Mixing procedures used with the Resodyn mixer evolved and improved throughout the project. Initial procedures were developed based on the equivalence ratio of 0.75. However, safety concerns related to the reactive nature of the nanoaluminum powder led to the decision of passivating the powder in air for two days prior to mixing. This passivation step lowered the active aluminum content by about 4% leading to an equivalence ratio closer to 0.71 and providing for a less reactive propellant. Again, the formulation studied here is far from optimum.

Strand burn experiments were performed using material from each mixing batch used to produce static fire grains. Each strand consisted of an 8 mm ID $\times$ 5 cm L tube filled with the $\phi = 0.71$ mixture. The frozen strand samples were

Table 1: Properties of 80 nm aluminum powder (Novacentrix Inc., product no. M2666).

Mean particle diameter, D_{av} (nm)			Lognormal probability distribution parameters		Oxide layer thickness, t_{av} (nm)		
D_{av}, BET[a]	D_{av}, SAS[b]	D_{av}[c]	Mean[c]	Std. Dev.[c]	t_{av}, SAS[b]	t_{av}, SSA[d]	t_{av}[c]
70	71 ± 7	79	4.25	0.481	2.4	2.34	2.54

[a] Per BET analysis as reported by Mang et al. [24].
[b] Per Small Angle Scattering analysis as reported by Mang et al. [24].
[c] Per SEM and TEM images analysis as reported by Sippel [25].
[d] Calculated from BET surface area and reported by Sippel [25].

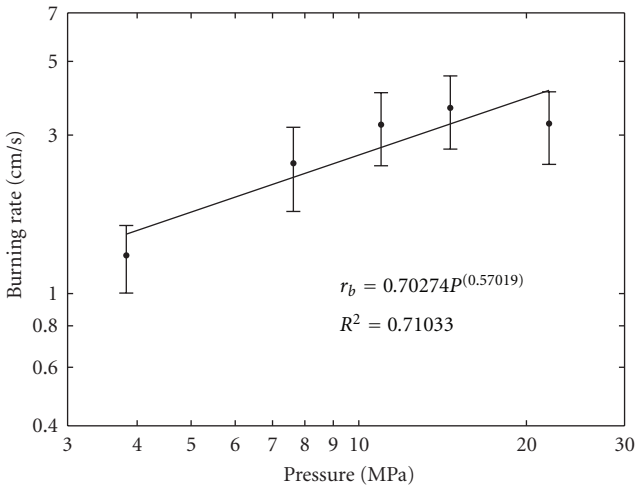

Figure 3: Burning rate data of ALICE propellant mixed with the Resodyn mixer.

burned in an argon pressurized and optically accessible combustion bomb. Burning rate measurements were repeated over a range of pressures leading to the power law estimate shown in Figure 3. Over 25 tests were performed and averaged in the results shown. The pressure exponent for this mixing procedure is 0.57, which is somewhat larger pressure dependency than the Al-water propellant tested by Risha et al. [17].

5. Motor Performance Prediction

An internal ballistics analysis of the combusting ALICE motor grain was developed using a lumped-parameter model. The control volume considered in this model takes into account the geometry of the experimental grains. These configurations are summarized in Table 2.

While a simple approach, the assumptions inherent to a lumped-parameter model are quite appropriate in the present application as the experimental grains had low aspect ratios L/D ranging from 1.2 for the 3.5″ long grains to 2.3 for the 7″ long grains, and, therefore, the pressure variations along the chamber length can be neglected [15]. Furthermore, while propellant and motor parameters are adjusted in the model, detail accounting of potentially important two-phase flow losses or nozzle flow losses is not within the scope of the present study. Instead, the model is used to predict the peak chamber pressure and thrust developed by the ALICE grains and to indicate the history of both parameters based on the measured burning rate and the geometry of the grain.

The ALICE propellant formulation assumed in the model has an equivalence ratio of 0.71 and a characteristic velocity of 1360 m/s. Further, based on previous experimental results reported and theoretical performance calculations, specific impulse of 210 s is assumed for the thrust calculations [26].

The results presented below include that of two variants of the model. In the first variant, the aforementioned propellant characteristics and nozzle geometries are assumed as nominal. It is used to predict the maximum thrust and chamber pressure prior to experimental testing of a new grain or chamber geometry. In the second variant, combustion and flow losses in the combustion chamber and through the nozzle are evaluated with model. These losses are taken into account in two ways: first, since posttest examination of the experimental hardware reveals alumina deposition on the throat and the expansion section of the nozzle, a simple deposition model is included in the analysis. The thickness of the alumina deposit is assumed to increase linearly with time up to the deposit thickness measured upon examination of the hardware. Second, performance losses are included by reducing the nominal propellant characteristic velocity and specific impulse values until a reasonable agreement with the experimental data is obtained.

A final simplifying assumption included in both variants of the model is that the total impulse and mass flow rate produced by the igniter are negligible compared to that of the ALICE grain. The validity of this assumption is discussed in the following. At any given instant in a lumped-parameter model, all exposed surfaces in the control volume are assumed to contribute to amount of mass produced by the combustion of the propellant:

$$\dot{m}_{in} = r_b \rho_p A_b. \tag{1}$$

Conversely, the mass flow exiting the nozzle is given by

$$\dot{m}_{out} = P_c \frac{A_t}{c^*}. \tag{2}$$

Combining (1) and (2) with the conservation of mass equation under steady-state conditions leads to

$$\frac{dm}{dt} = 0 = \dot{m}_{in} - \dot{m}_{out} = r_b \rho_p A_b - P_c \frac{A_t}{c^*}. \tag{3}$$

Table 2: ALICE grain geometries.

Test	Grain dimensions			Casing dimensions	
	Outer diameter (cm/in)	Inner bore diameter (cm/in)	Length (cm/in)	Chamber length (cm/in)	Nozzle throat diameter (cm/in)
1 to 3	7.62/3	2.54/1	8.89/3.5	12.70/5	0.914/0.36
4 to 5	7.62/3	2.54/1	12.70/5	12.70/5	1.067/0.42
6	7.62/3	2.54/1	17.14/6.75	19.05/7.5	1.321/0.52
7	7.62/3	2.54/1	17.78/7	19.05/7.5	1.321/0.52

Equation (3) can then be solved for the chamber pressure using St-Robert's burning rate law, $r_b = aP_c{}^n$:

$$P_c = \left(\frac{a\rho_p A_b c^*}{A_t}\right)^{1/(1-n)}. \quad (4)$$

Since neither end of the grain is inhibited, the ALICE grain burning surface area is a function of the grain outer and inner bore diameter and the grain length as given by

$$A_b = 2\pi R_i L + 2\left(\frac{\pi}{4}(2R_o)^2 - \frac{\pi}{4}(2R_i)^2\right), \quad (5)$$

with both R_i and L functions of the web thickness consumed normal to the local burn surface. The web thickness, W, can therefore be defined as the integral of the burning rate history as given by

$$W = \int_o^{t_b} r_b(t)dt. \quad (6)$$

The theoretical mass flow rate and thrust can then be calculated based on (1) or (2) and

$$F = g \cdot I_{\text{sp}} \cdot \dot{m}_{\text{in}}. \quad (7)$$

Both variants of the lumped parameter model incorporate (1) to (7) using an Euler numerical integration method with an adequately small time step (typically 1 ms). The second model variant reflects the previously mentioned performance losses and the alumina deposition on the nozzle according to (8):

$$D_t = D_t - 2\varepsilon dt, \quad (8)$$

where ε is the thickness of the alumina deposit measured around the circumference of the nozzle throat. The chamber pressure and thrust profiles calculated with both variants of the model are shown in Table 3 and Figure 5 for a 5″ long ALICE grains.

As shown in Table 3, a peak chamber pressure of ~14.5 MPa is calculated with both variants of the model. However, the peak pressure obtained with the second variant follows a longer chamber pressurization period and occurs a quarter of a second later than with the first variant (Figure 5). This delay is a result of the reduced characteristic velocity, assumed to be 85% of nominal in the second model variant. The peak pressures calculated with both variants are almost identical as a result of the assumed alumina deposition model.

Also shown in Table 3 is the reduction in peak thrust from ~2 to ~1.78 kN from the first to the second variant of the model. This reduction is the result of the lower specific impulse value assumed in the second variant of the model.

6. ALICE Battleship Static Thrust Stand Experiments

Several static rocket tests were conducted in the Purdue University Propulsion laboratory. The test cell for the static tests has a remote control room from which experiments are monitored and initiated. Pressure and thrust are recorded using LabView, and a 16-bit National Instruments, 32 channel data acquisition system. At least two video cameras are used to observe and record the experiments. One camera monitors the outside where the plume is expelled, and another high-speed camera, recording at 300 fps, monitors the side profile of the exhaust plume.

Based on the strand burn tests, the ALICE propellant combustion does not perform well at pressures below 7 MPa; therefore a thick steel "battleship" motor casing was used initially (see Figure 4). This casing was sized to withstand internal pressures up to 35 MPa. However, constraints in the design of the flight-weight casing influenced the operating pressure of ALICE to be below 20 MPa. To eliminate an additional variable between the battleship tests and the flight-weight tests, the same bolts were selected to secure the ALICE motor assembly together. These bolts are designed to fail around 22 MPa, so overpressurization does not result in the failure of the casing. With the anticipation that variations in mixing and casting will affect performance, the nozzle throat diameter was varied to provide a peak chamber pressure of 10–14 MPa.

The battleship casing was attached horizontally to a metal stand frame. The metal framing is attached to a pair of flexures, which transfers the thrust to a 4.5 kN load cell (Interface, Scottsdale, Arizona). Chamber pressure is measured using two PMP 1260 diaphragm pressure transducers, (Druck, GE Electrics, Billerica, MA) with a 0.25% full-scale accuracy.

Following a few experimental tests with various igniter motor sizes, the igniter of choice in all test configurations was a commercially available Aerotech H180 motor [27]. A summary of the motor specifications of interest in the present study is provided in Table 4. The reported I_{SP} of 178 s is not unexpected for small motors such as these. As listed in Table 4, the Aerotech H180 motor has a total impulse of

Table 3: Modeling summary for 5″ long grain.

Model assumptions	Total impulse (N-s)	Peak P_c (MPa)	Peak thrust (kN)
No losses for 5″ long grain	1484	14.68	1.98
With deposit and losses for 5″ long grain	1336	14.82	1.78

Table 4: Aerotech H180 motor specifications [27].

Parameter	Value	Unit
Outer diameter	29.0	mm
Total length	23.8	cm
Total weight	252	g
Propellant weight	124	g
Average thrust	180.0	N
Maximum thrust	228.5	N
Total impulse	217.7	N-s
Burn time	1.3	s
I_{sp}	178	s

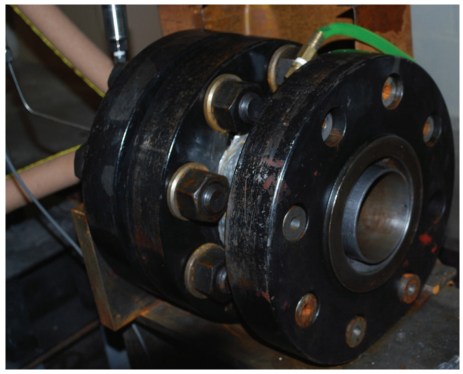

Figure 4: Photograph of the battleship motor casing for 3″ diameter propellant grains.

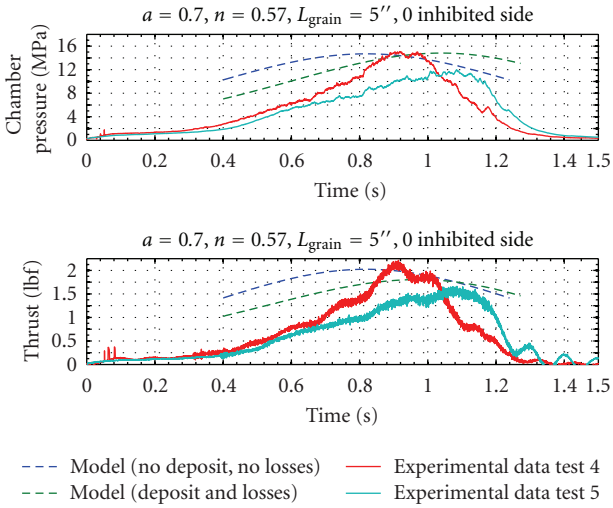

Figure 5: Comparison of 5″ long ALICE motor tests with lumped parameter models.

218 N-s or about 15% of the total impulse predicted with the first variant of the lumped parameter model for a 5″ long ALICE grain (Table 3). While a smaller igniter would be highly desirable, the selected igniter size was necessary for reliable and fast ignition of the ALICE formulation evaluated in the study.

Several runs were performed with the battleship motor. Initial runs started with 3.5″ long grains. The results of these experiments are not presented herein for conciseness. Following three successful runs with the 3.5″ long grains, the length of the grain was increased to 5″ to provide more thrust and better approximate the scale required for the sounding rocket. The experimental results of the two runs performed with 5″ long grains (Tests 4 and 5) are presented and compared with the modeling results in Figure 5 and Table 5.

Although the two tests are not precisely replicated, there are several key features to note. First, the length and packing densities of both 5″ long grains varied by 2.3% and 4.8%, respectively, with the first 5″-class grain about 0.25 inches longer than the second one. Second, while aluminum agglomeration on the nozzle or variations in casting could explain the differences in peak pressure, the experimental peak pressures and peak thrusts compare well with the modeling results thus providing an increased level of confidence for performance prediction of longer grains. The experimental and modeling results obtained for the 5″-class grains are provided in Table 5 including the calculated total impulse values which are of particular interest for the sounding rocket trajectory predictions.

Shown on Figure 6 is the recorded thrust profile for Test 4 and images of the plume at selected time stamps during the burn. The first picture (Figure 6(A)) is the start of the igniter flame and initial chamber pressurization. As the H-180 igniter motor burns, gases expand in the ALICE casing and exit the nozzle as a dark smoke. Based on the recorded data (pressure and thrust), it is believed that ALICE begins to burn in the second picture (Figure 6(B)). This is evident from the sudden oscillatory change in thrust from the load cell, that has been consistent throughout the battleship tests. As the pressure increases further, the flame continues to increase in size until the peak pressure is reached (Figures 6(B) to 6(F)). The pressure and thrust decay rapidly following the consumption of the ALICE grain.

7. Rocket Design and Launch

The demonstration flight of the ALICE propellant with an unguided experimental rocket was a proof of concept for more advanced rockets using similar nanoenergetic material-based propellants. The flight followed a rigorous design

Table 5: Comparison of modeling and experimental results for 5″ long grains.

	Total impulse (N-s)	Peak P_c (MPa)	Peak thrust (kN)
Model with no losses (5″ long grain)	1484	14.68	1.98
Model with deposit & losses (5″ long grain)	1336	14.82	1.78
5″ Long experimental grain (Test 4)	970	14.89	2.13
5″ Long experimental grain (Test 5)	890	11.72	1.56

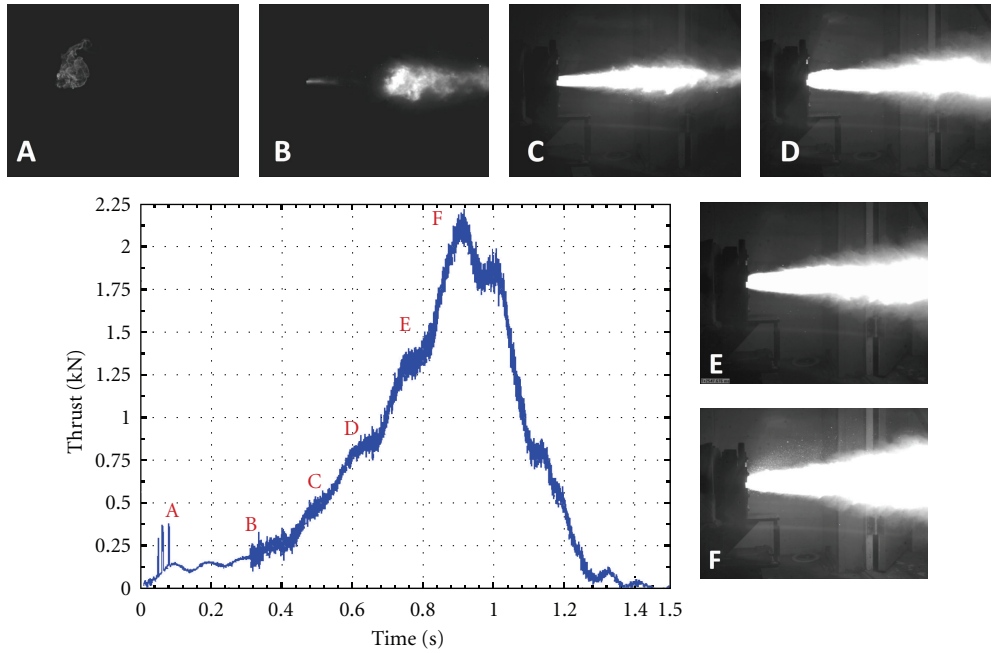

Figure 6: Thrust profile of Test 4 and corresponding plume images recorded by the high-speed camera.

process and extensive ground testing of the ALICE rocket motor thus minimizing the likelihood of ignition issues or motor structural failure.

The experimental rocket chosen for the flight is an all-carbon-fiber, minimum diameter, 98 mm high-power rocketry kit known as a Mongoose 98. Two launches were performed with this rocket; the first flight used a K-780 commercially available rocket motor to test the avionics bay and deployment of the parachutes, and the second used the flight-weight motor casing with an ALICE propellant grain. All launch operations were carried out at a remote area located approximately 12 miles southwest of West Lafayette. Known as Scholer Farm, this land is owned by Purdue University and managed by the Animal Sciences Research and Education Center (ASREC). The first flight, with the K780 commercial motor, took place on June 14th, 2009. The demonstration flight of the ALICE propellant took place approximately two months later on August 7th, 2009. For both test flights, we used a commercial ballistic trajectory simulation code (Rocsim-PRO, [28]) to calculate flight-vehicle performance (altitude, range, velocity, and acceleration). This code simulates flight with the addition of wind speed and direction, atmospheric thermal gradients, pressure, location latitude/longitude, launch rail azimuth/elevation, and more. In addition it incorporates the NASA SPLASH code in order to perform 6-DOF Monte-Carlo simulations based on the uncertainty values in physical parameters such as mass properties (moment of inertia, center-of-gravity), aerodynamics (drag coefficient, center-of-pressure, fin cant angle), propulsion (total impulse, propellant mass, thrust axis), wind direction/velocity, and launch guide angle uncertainties.

Shown in Figure 7, the ALICE flight-vehicle is composed of two fuselage sections, connected together by a carbon-fiber interstage coupler and an avionics bay which contain two redundant R-DAS (Rocket Data-Acquisition System) Tiny units (AED Electronics; The Netherlands). The R-DAS units are preprogrammed to eject a drogue parachute at apogee and a main parachute at a predetermined altitude. An ogive nose cone is placed on the forward end of the vehicle, and three carbon-fiber fins are attached to the aft end in order to provide aerodynamic stability. The fins are attached with carbon-fiber plain weave cloth by using a wet hand layup technique to apply the cloth from fin-tip to fin-tip. Following the layup process, vacuum bagging is used to provide pressure on the composite layer assembly in order to remove any excess resin and improve bond strength.

The flight weight motor and igniter casings shown schematically in Figure 8 are built out of solid rods of 7075-T6 aluminum. This method is preferred over welding on

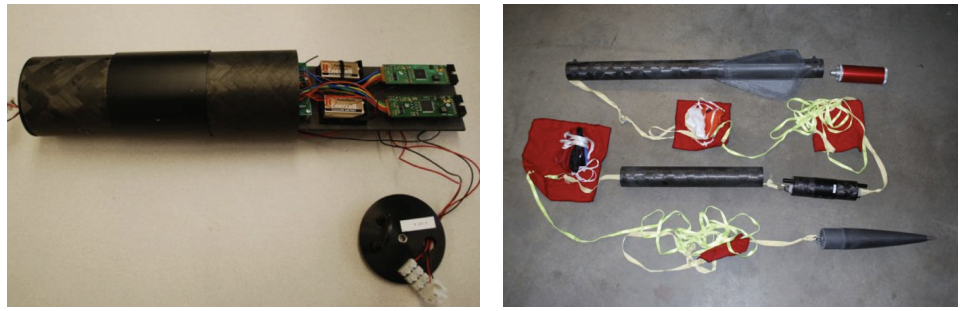

(a) (b)

Figure 7: Images of the sounding rocket: (a) altimeter bay with RDAS units; (b) exploded view of Mongoose 98 Rocket. The entire length of the assembled rocket is about 8 feet 6 inches and the outside diameter is 4″.

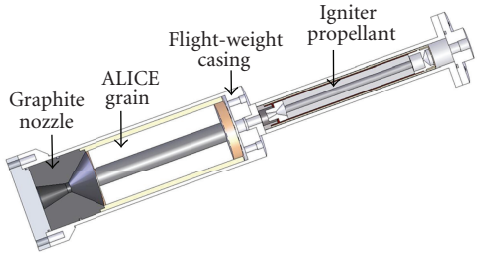

Figure 8: Schematic of the flight-weight motor casing.

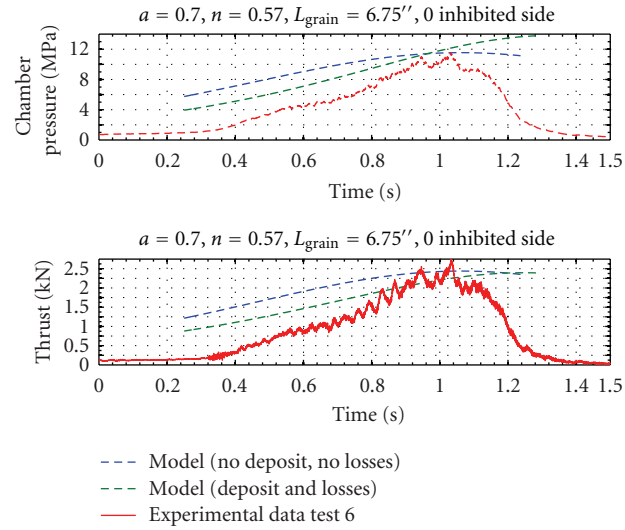

Figure 9: Comparison of 7″ long ALICE motor tests with lumped parameter models.

flanges to the end of the casing, which could potentially cause changes in the mechanical properties of the aluminum. Bolts are threaded into steel threaded inserts located in the aluminum flange at the aft end of the motor casing. These steel inserts help to distribute the load evenly over the length of the thread. The bolts are the same ones used on the battleship motor, which were selected to fail at 22 MPa. The results of a structural analysis of the flight-weight motor using a 3D ProMechanica model with a solid mesh of 3512 elements and an 18 MPa internal pressure load lead to a failure index of 0.29 based on the tensile yield strength of aluminum 7075-T6 of 500 MPa. Upon completion of the casing, the vessel was hydrotested for several minutes at a pressure of 14 MPa. Passing this test allowed for the first static test with the ALICE propellant.

Two static fire tests were conducted with the flight-weight hardware prior to launch. The first test (Test no. 6 in Table 2) was performed with the horizontal configuration established with the battleship motor. The last static test prior to launch (Test no. 7 in Table 2) was performed with the motor installed vertically to assess how the grain and alumina slag would behave under the effects of gravity. These concerns ranged from questions on whether the grain would become dislodged from the walls of the phenolic tube and slide toward the nozzle or if the alumina slag would clog the nozzle. This vertical test was conducted using the same Aerotech H180 igniter as in prior tests. The grain was slightly longer, from 6.75″ to 7″, compared to the previous horizontal test but with a nearly identical packing density (within 2.2%). Figure 9 displays the experimental data of the vertical test and the predictions obtained with the performance prediction model. Using the previously described simplifying assumptions for alumina deposition, characteristic velocity and specific impulse losses, the second variant of the model reflects the progressive nature of the grain burning but overpredicts the peak chamber pressure.

Based on the thrust profile from the hot-fire test performed with the 7″ long ALICE grain, as well as the new flight-weight motor design, the Rocsim-PRO simulations predicted that the 30 lb flight vehicle would depart the launch rail in 0.9 seconds, achieving a velocity of ~20 m/s at rail exit. The simulations also predicted a maximum acceleration of 16 G's, maximum velocity of ~300 km/h (Mach 0.24), and a nominal altitude of ~365 m under no wind conditions.

Several constraints limited the achievable altitude with the current ALICE powered rocket. First, the combustion and flow losses observed during the last six static test firings lead to total impulse values of about 60% that of the predicted values. These losses are being addressed in ongoing work with improved propellant formulations

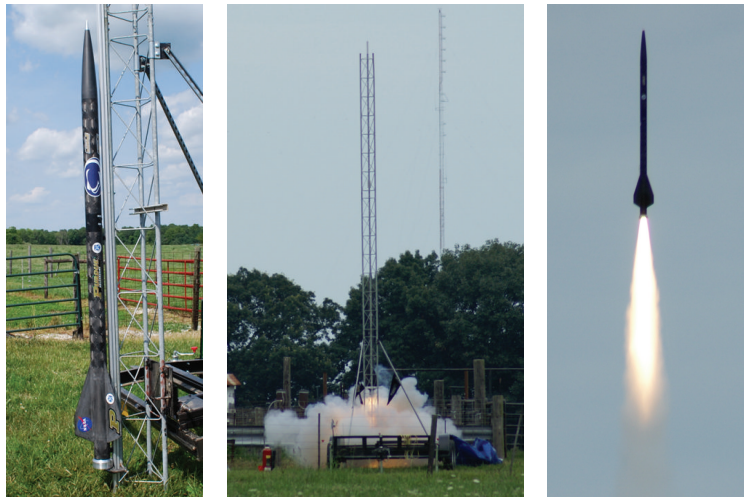

(a) (b) (c)

Figure 10: Images from the ALICE flight test: rocket on launch platform (a), ignition of the ALICE propellant (b), and rocket in flight (c).

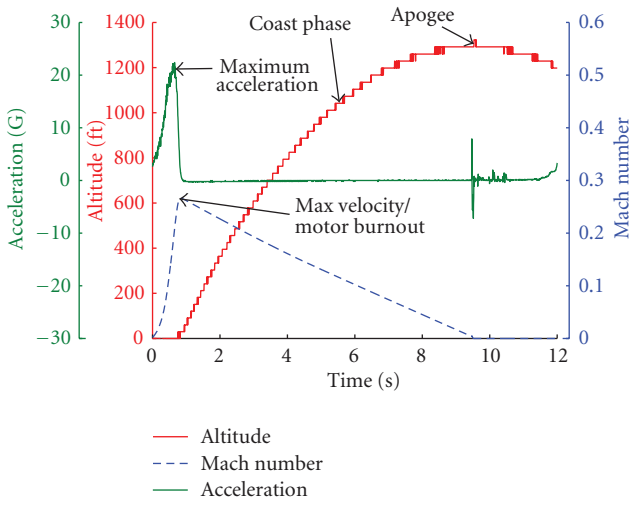

Figure 11: R-DAS flight-data from test launch of the flight vehicle powered by the ALICE motor.

including additives and alternative formulations to achieve higher specific impulse and lower the alumina content of the products. Second, the flight-weight casing for the ALICE propellant had to sustain pressures up to 14 MPa requiring thicker walls, thus increasing vehicle weight compared to a traditional SRM. In addition, the energy required for igniting the current ALICE propellant formulation is significantly higher than that required for a standard solid propellant. This leads to added weight for an igniter casing and an interface with the ALICE casing capable of sustaining high pressures and designed in such a way that the combustion gases do not impact the aluminum walls. Weights were also added just below the nose cone to yield a higher stability margin. While designed for flight with safety factors around 1.5, the heavier casing reduced the maximum altitude achievable with the rocket. Finally, the burning rate of the current ALICE formulation is on the order of 2.5 cm/s at the nominal operating pressure of 10 MPa. This high burning rate means that a larger web thickness is required to sustain the ALICE combustion over sufficiently long durations. In turn, larger grains require heavier casings. The current design is a trade-off between the aforementioned constraints. Further improvements of the propellant formulation should address these constraints, thus reducing the weight of the flight-weight casing in an effort to achieve better flight performance.

The ALICE demonstration flight took place of a fairly cool (~21°C ambient temperature) and calm (~3 km/h wind at launch site) day.

Figure 10 shows the ALICE vehicle on the stand ready for takeoff (left), soon after ignition (middle), and flying under ALICE soon after it cleared the launch tower (right).

The rocket coasted after the grain was depleted and reached a peak altitude of ~394 m (1292 ft). This altitude is very close to the estimate of 365 m (1200 ft) obtained from Rocsim-PRO assuming no wind. The data recorded from the R-DAS is shown in Figure 11.

This close agreement between recorded flight data and predictions indicates that the thrust profile and thrust magnitude experienced during flight were very similar to those recorded on the ground with the flight hardware. Similarly, it is observed that the peak I_{sp} of 210 s calculated from the ground test data is a good estimate for the flight I_{sp}.

8. Conclusions

We have shown that refrigerated solid propellants can be used for rocket motors, and the ALICE propellant has shown promise as a rocket propellant in static test firings. Six small-scale static experiments have shown consistent results when compared to the prediction codes. Although this current propellant formulation is far from optimized, improvements in the mixing procedure have produced a consistent and

homogeneous propellant. While the performance of ALICE is too low for practical use, the knowledge gained through formulating and experimenting with nanoscale particles in a simple mixture is of great interest for ongoing research activities on advanced propellants.

An internal ballistic model developed to support the experiments provides a simplified account of a complex series of events within the igniter and the main combustion chamber. The model is based on measured burning rate parameters and exact grain geometries tested at the Purdue Propulsion Laboratories. Perturbations to the model can be introduced to reflect the reduction of the nozzle throat diameter due to alumina deposition and to take into account losses in the combustion chamber and the nozzle. While the model overpredicts the total impulse of the ALICE propellant grains, it is a useful tool for peak chamber pressure and thrust predictions. Finally, based on consistency between model and experiment over several tests, the model is also a prediction tool for flight-weight motor performance and, therefore, rocket trajectory predictions.

Nomenclature

a, n: Propellant burning rate coefficients
A_b: Burning area
A_t: Throat area
c^*: Characteristic velocity
D_{av}: Average particle diameter
D_t: Throat diameter
dt: Time increment
F: Thrust
g: Gravity
I_{sp}: Specific impulse
L: Length
m: Mass
$\dot{m}$: Mass flow rate
P_c: Chamber pressure
r_b: Burning rate
R_o: Outer diameter
R_i: Inner diameter
t_{av}: Oxide layer thickness
t_b: Burning time
W: Web thickness
ε: Thickness of alumina deposit
ρ_p: Propellant density
ϕ: Mixture ratio.

Subscript

in: In
out: Out
p: Propellant.

Acknowledgments

The authors would like to thank Dr. Mitat Birkan of the Air Force Office of Scientific Research and NASA under contract numbers FA9550-09-1-0073 and FA9550-07-1-0582. The authors would also like to thank Mr. T. L. Connell, Jr., Dr. Grant A. Risha and Dr. Richard A. Yetter of the Pennsylvania State University for their many contributions.

References

[1] K. K. Kuo, G. A. Risha, B. J. Evans, and E. Boyer, "Potential usage of energetic nano-sized powders for combustion and rocket propulsion," *Materials Research Society Symposium Proceedings*, vol. 800, pp. 3–14, 2003.

[2] A. Dokhan, E. W. Price, J. M. Seitzman, and R. K. Sigman, "The effects of bimodal aluminum with ultrafine aluminum on the burnign rates of solid propellants," *Proceedings of the Combustion Institute*, vol. 29, no. 2, pp. 2939–2946, 2002.

[3] A. Shalom, H. Aped, M. Kivity, and D. Horowitz, "The effect of nanosized aluminum on composite propellant properties," in *Proceedings of the 41st AIAA/ASME/SAE/ASEE Joint Propulsion Conference and Exhibit*, July 2005.

[4] L. Galfetti, F. Severini, L. T. De Luca, and L. Meda, "Nano-propellants for space propulsion," in *Proceedings of the 4th International Spacecraft Propulsion Conference*, vol. 4, Sardinia, Italy, June 2004.

[5] M. A. Trunov, M. Schoenitz, and E. L. Dreizin, "Ignition of aluminum powders under different experimental conditions," *Propellants, Explosives, Pyrotechnics*, vol. 30, no. 1, pp. 36–43, 2005.

[6] G. A. Risha, Y. Huang, R. A. Yetter, V. Yang, S. F. Son, and B. C. Tappan, "Combustion of aluminum particles with steam and liquid water," in *Proceedings of the 44th AIAA Aerospace Sciences Meeting and Exhibit*, January 2006.

[7] V. G. Ivanov, M. N. Safronov, and O. V. Gavrilyuk, "Macrokinetics of oxidation of ultradisperse aluminum by water in the liquid phase," *Combustion, Explosion and Shock Waves*, vol. 37, no. 2, pp. 173–177, 2001.

[8] A. Ingenito and C. Bruno, "Using aluminum for space propulsion," *Journal of Propulsion and Power*, vol. 20, no. 6, pp. 1056–1063, 2004.

[9] E. Shafirovich, P. E. Bocanegra, C. Chauveau, and I. Gökalp, "Nanoaluminium—water slurry: a novel "green" propellant for space applications," in *Proceedings of the 2nd International Conference on Green Propellants for Space Propulsion*, vol. 2, Sardinia, Italy, June 2004.

[10] O. Rasor and O. R. Portland, U.S. Patent Application for a "Power Plant", 1939.

[11] O. J. Elgert and A. W. Brown, *In Pile Molten Metal-Water Reaction Experiment*, U.S. Atomic Energy, 1956.

[12] L. Leibowitz and L. W. Mishler, "A study of aluminum-water reactions by laser heating," *Journal of Nuclear Materials*, vol. 23, no. 2, pp. 173–182, 1967.

[13] T. F. Miller and J. D. Herr, "Green rocket propulsion by reaction of Al and Mg powders and water," in *Proceedings of the 40th AIAA/ASME/SAE/ASEE Joint Propulsion Conference and Exhibit*, July 2004.

[14] J. P. Foote, J. T. Lineberry, B. R. Thompson, and B. C. Winkelman, "Investigation of aluminum particle combustion for underwater propulsion applications," in *Proceedings of the 32nd AIAA/ASME/SAE/ASEE Joint Propulsion Conference and Exhibit*, 1996.

[15] R. W. Humble, G. N. Henry, and W. J. Larson, *Space Propulsion Analysis and Design*, chapter 6, McGraw-Hill, New York, NY, USA, 1st edition, 1995.

[16] V. G. Ivanov, O. V. Gavrilyuk, O. V. Glazkov, and M. N. Safronov, "Specific features of the reaction between ultrafine

aluminum and water in a combustion regime," *Combustion, Explosion and Shock Waves*, vol. 36, no. 2, pp. 213–219, 2000.

[17] G. A. Risha, S. F. Son, R. A. Yetter, V. Yang, and B. C. Tappan, "Combustion of nano-aluminum and liquid water," *Proceedings of the Combustion Institute*, vol. 31, no. 2, pp. 2029–2036, 2007.

[18] T. R. Sippel, S. F. Son, G. A. Risha, and R. A. Yetter, "Combustion and characterization of nanoscale aluminum and ice propellants," in *Proceedings of the 44th AIAA/ASME/SAE/ASEE Joint Propulsion Conference and Exhibit*, July 2008.

[19] A. Dokhan, *The effects of aluminized particle size on aluminized propellant combustion [Ph.D. thesis]*, Aeronautics and Astronautics Department , Georgia Institute of Technology, Atlanta, Ga, USA, 2002.

[20] Y. S. Kwon, A. A. Gromov, and J. I. Strokova, "Passivation of the surface of aluminum nanopowders by protective coatings of the different chemical origin," *Applied Surface Science*, vol. 253, no. 12, pp. 5558–5564, 2007.

[21] M. Cliff, F. Tepper, and V. Lisetsky, "Ageing characteristics of Alex nanosize aluminum," in *Proceedings of the 37th AIAA/ASME/SAE/ASEE Joint Propulsion Conference and Exhibit*, 2001.

[22] C. Franson, O. Orlandi, C. Perut et al., "Al/H_20 and Al/H_20/H_20_2 frozen mixtures as examples of new composite propellants for space application," in *Proceedings of the 7th International Symposium on Launcher Technologies*, Barcelona, Spain, 2007.

[23] LabRam Resonant Acoustic Mixer Manual, ResoDyn, Butte, Mont, USA, 2012 http://www.resodynmixers.com/products/labram/.

[24] J. T. Mang, R. P. Hjelm, S. F. Son, P. D. Peterson, and B. S. Jorgensen, "Characterization of components of nanoenergetics by small-angle scattering techniques," *Journal of Materials Research*, vol. 22, no. 7, pp. 1907–1920, 2007.

[25] T. R. Sippel, *Characterization of nanoscale aluminum and ice solid propellants [M.S. thesis]*, Mechanical Engineering Department, Purdue University, West Lafayette, Ind, USA, 2009.

[26] R. A. Yetter, G. A. Risha, T. Connell et al., "Novel energetic materials for space propulsion," in *Presentation, AFOSR/NASA Office of Chief Engineer Joint Contractors / strategic Planning Meeting in Chemical Propulsion*, Vienna, Va, USA, 2008.

[27] ThrustCurve, John Coker, 2012, http://www.thrustcurve.org/.

[28] "RockSim, Ver. 8.0," Apogee Components, Inc., Colorado Springs, Colo, USA, 2009.

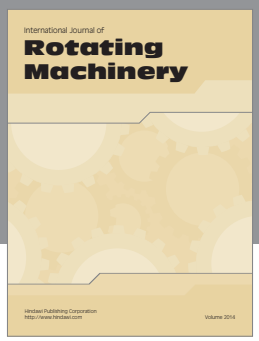

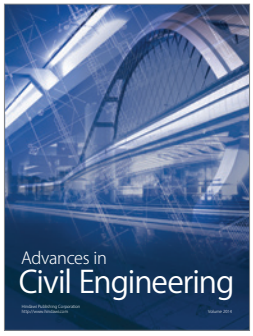

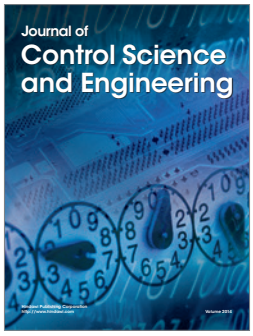

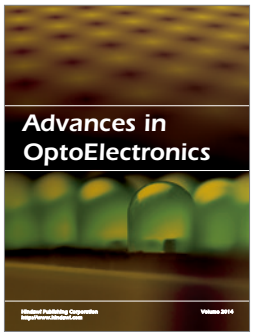

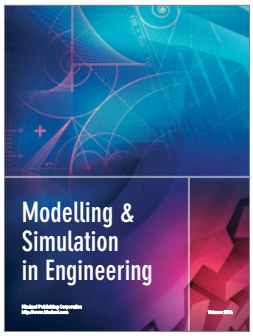

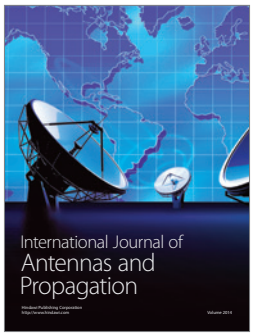

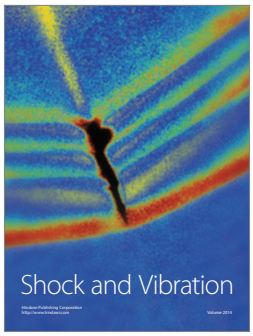

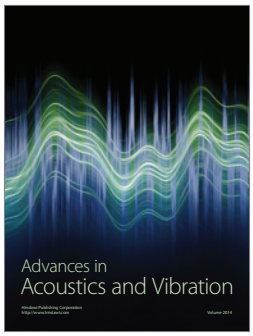

Hindawi

Submit your manuscripts at
http://www.hindawi.com